Contents lists available at GrowingScience

Engineering Solid Mechanics

homepage: www.GrowingScience.com/esm

Thermoelastic micro-stretch solid immersed in an infinite inviscid fluid and subject to a rotation under two theories

Mohamed I.A. Othman[a*], Ebtesam E.M. Eraki[a], Sarhan Y. Atwa[b] and Mohamed F. Ismail[b]

[a]*Department of Mathematics, Faculty of Science, Zagazig University, P.O. Box 44519, Zagazig, Egypt*
[b]*Department of Mathematics Engineering of Physics, Higher Institute of Engineering, Shorouk Academy, Shorouk City, Egypt*

ARTICLE INFO

Article history:
Received 16 August 2022
Accepted 2 February 2023
Available online
2 February 2023

Keywords:
Microstretch thermoelastic
Normal mode method
Rotation
Fluid
Frequency

ABSTRACT

This work is interested with a thermoelastic response in a micro-stretch half-space submerged in an unlimited non-viscous fluid under rotation, the medium is studied using the theory of Green-Naghdi (G-N III) and the model of three-phase-lag (3PHL). The governing equations are formulated in the context of G-N theory and the 3PHL model. Analytical solution to the problem is acquired by utilizing the normal mode method. The magnesium crystal element is utilized as an application to compare the predictions induced by rotation on microstretch thermoelastic immersed in an infinite fluid of G–N theory with those for the 3PHL model. Rotation has been noticed to have a major effect on all physical quantities. Comparisons were also made for three values of wave number b and three values of the real part frequency ω_0.

Nomenclature

$\boldsymbol{u}$ Displacement vector in micro-elongated medium
e Dilatation
τ_v Phase lag of thermal displacement gradient
Ω Rotation
c_E Specific heat at the constant strain
φ_i Micro-rotation vector
$k, \alpha, \beta, \gamma, \alpha_0, \lambda_0, \lambda_1$ are material constant
φ^* Scalar microstretch function
j_0 Micro-inertia of microelement
σ_{ij} Component of stress tensor
m_{ij} Component of couple stress tensor
j Micro-inertia
k^* Additional material
λ, μ Lame's constants
k_1^* Thermal conductivity
ε_{ijr} Alternate tensor
τ_θ The temperature gradient phase lag
τ_q The heat flux phase lag
ρ Density for microstretch
δ_{ij} Kronecker delta
$\boldsymbol{u}^f$ Displacement vector for fluid
λ^f The bulk modulus
σ_{ij}^f Component of stress tensor of fluid
ρ^f Density of the fluid
c_1^f The velocity of sound of the fluid
$\alpha_{t_1}, \alpha_{t_2}$ linear thermal expansion coefficient where $\beta_1 = (3\lambda + 2\mu + k)\alpha_{t_1}$, $\nu = (3\lambda + 2\mu + k)\alpha_{t_2}$

* Corresponding author.
E-mail addresses: m_i_a_othman@yahoo.com (M. I.A. Othman)

ISSN 2291-8752 (Online) - ISSN 2291-8744 (Print)

doi: 10.5267/j.esm.2023.2.002

1. Introduction

Many media, such as animal bones, solids with micro-cracks, porous media with gas-filled pores, foams, and inviscid fluids, fall just outside the domain of micropolar elasticity. As a result, scientists needed to develop a mathematical model to study these media, and they chose microstretch as a mathematical model for these types of solids. There are seven degrees of freedom in microstretch elastic solids: three in rotation, three for translation, and one for the stretch. Microstretch bodies' material points can extend and shrink independently of translation and rotating. Sharma et al. (2007) examined the spreading of generalized Rayleigh surface waves in an isotropic, homogeneous, thermo-elastic micro-stretch solid half-space underlying a non-viscous fluid half-space in the context of classical and non-classical thermoelasticity theories. Kumar and Partap (2009) discussed the development and spread of free vibrations in a micro-stretch thermoelastic isotropic homogeneous thermodynamically conducting plate bordered on both sides by layers of an inviscid fluid, using the thermoelastic theories of the Lord and Shulman (L-S) and the Green and Lindsay (G-L). The spreading of straight and round crested waves in micro-stretch thermoelastic plates bounded by inviscid fluid layers with different temperatures on two sides using generalized thermo-micro-stretch elasticity theory was examined by Kumar et al. (2011). Xu et al. (2011) studied a model based on fluid-structure interaction theory to describe the thermoelastic generation with laser and spreading of Leaky Lamb waves at the interface of water-aluminum. Kumar et al. (2014) explored the spreading of Rayleigh-type surface waves in a micro-stretch thermoelastic homogeneous diffusion medium half-space with just a layer of non-viscous fluid. The phenomenon of refraction and reflection at a plane interface among a non-viscous liquid medium and a micro-stretch thermoelastic diffusion, medium is studied by Kumar (2014). Othman and Ismail (2015) employed the Lord-Shulman theory and the DPL model to investigate the impact of gravity on a micro-elongated thermoelastic solid under the fluid load. Deswal et al. (2022) examined the reflection of waves at the free surface of a nonlocal micro-stretch thermoelastic medium under the model of 3PHL with temperature-dependent properties.

Othman and Atwa (2014) utilized the theory of Green-Naghdi to discuss the influence of gravity and rotating reinforcement on overall body deformation and their mutual interaction. Marin and Öchsner (2018) examined an initial boundary value problem for modeling a piezo-electric dipolar body. Abouelregal et al. (2021) researched thermo-photovoltaic interactions employing a new thermoelasticity mathematical model based on a modification of the G-N theory of type III. Kutbi and Zenkour (2021) proposed four thermoelasticity models that could be applied to simulate thermomechanical waves in an axisymmetric rotating disc. Youssef and El-Bary (2022) designed a novel mathematical formula for a semiconducting solid sphere focused on photo-thermal interaction in the context of the three G-N models: type-I, type-II, and type-III. Lata and Himanshi (2022) studied the impact of the fractional order parameter in a 2D orthotropic magneto-thermo-elastic plate in generalized thermo-elasticity employing the Green-Naghdi model of type II with fractional order heat transfer throughout the context of hall current, two-temperature and rotation due to normal force.

Roy Choudhuri (2007) established a neoteric theory known as the 3PHL model for a heat transport mechanism in which the Fourier law is replaced by a strategy to a modification of the Fourier law with different time's translations for the heat flux, temperature gradient, and thermal displacement gradient. Kumar and Chawla (2011) examined the spreading of plane waves in anisotropic thermoelastic media utilizing 3PHL and DPL thermoelastic models. One-dimensional thermoelastic disturbances in an unlimited, isotropic, functionally graded thermo-viscoelastic medium in the background of G-N model II, G-N model III and the 3PHL thermoelastic models, in the existence of variated periodically different heat sources is examined by Sur and Kanoria (2014). After five years, the previous theories are used to study two-temperature fiber-reinforced thermoplastic isotropic medium with the effect of gravity field by Othman et al. (2019). Sharma et al. (2021) explored the influence of the 3PHL generalized thermoelastic model on the perfect evaluation of 3D free vibrations of a viscous thermoelastic solid cylinder that is supposed to be undeformed at first and at a uniform temperature. In the context of the model of 3PHL, Othman and Abbas (2021) investigated the 2D deformation of the thermoelastic micropolar plate with the rotation utilizing the model of 3PHL. Marin et al. (2020) studied the structural stability for an elastic body with voids having dipolar structure. The normal mode method was applied to find the solution to the 2D distortion of the thermoelastic micro-elongated plate under the initial stress and one relaxation time on the model of DPL introduced by Othman et al. (2021). Several authors studied about generalized thermoelastic materials by using the normal mode method which can be found in some references (Marin et al., 2022; Othman et al., 2021; Sur, 2022; Miszuris & Öchsner, 2013; Abouelregal et al., 2022).

In this work, we focused our attention to explore the thermoelastic response in a micro-stretch thermoelastic half-space submerged in an unlimited non-viscous fluid under rotation as shown in Fig. 1, the medium is studied using the G-N theory and the 3PHL model. We started by explaining the basic equations and using non-dimensions. In the second, we employed the normal mode method to convert the partial differential equations to the ordinary differential equations. Afterward, we establish the boundary conditions at $z = \pm d$ to discover the constant values of the solutions. Finally, the numerical results are put into practice, debated, and graphed.

2. The description of the problem and basic equations

In a 3PHL model, the system of governing equations of a microstretch thermoelasticity can indeed be expressed as (Kumar et al., 2014; Kumar & Chawla, 2011; Singh & Singla, 2020).

The equation of motion

$$\sigma_{ji,j} = \rho\,[\,u_{i,tt} + \{\boldsymbol{\Omega}\times(\boldsymbol{\Omega}\times\boldsymbol{u})\}_i + (2\boldsymbol{\Omega}\times\boldsymbol{u}_{,t})_i\,]. \tag{1}$$

The equation of micropolar

$$\varepsilon_{ijr}\sigma_{jr} + m_{ji,j} = \rho j\,[\varphi_{i,tt} + \boldsymbol{\Omega}\times\boldsymbol{\varphi}_{,t}\,] \tag{2}$$

The equation of micro-stretch

$$\alpha_0\varphi^*_{,ii} + \frac{1}{3}\nu T - \frac{1}{3}\lambda_1\varphi^* - \frac{1}{3}\lambda_0 u_{,i} = \frac{3}{2}\rho j_0\varphi^*_{,tt}. \tag{3}$$

The equation of heat under 3PHL model

$$k^* T_{,ii} + (k_1^* + k^*\tau_\nu)\,T_{,t} + k_1^*\tau_\theta\,T_{,ttii} = [1 + \tau_q\frac{\partial}{\partial t} + \frac{1}{2}\tau_q^2\frac{\partial^2}{\partial t^2}][\rho c_E T_{,tt} + \nu T_0\varphi^*_{,tt} + \beta_1 T_0 e_{,tt}\,], \tag{4}$$

where, G-N theory of type III, when ($\tau_\nu = \tau_\theta = \tau_q = 0,\ k^* > 0$).

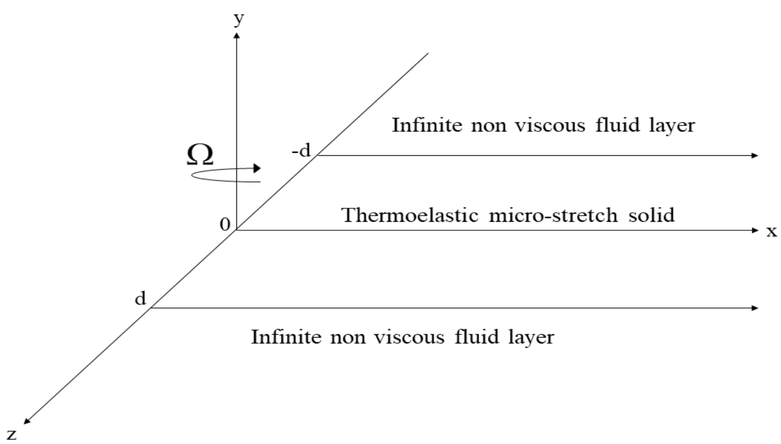

Fig. 1. Geometry of problem.

The constitutive relations

$$\sigma_{ij} = (\lambda u_{r,r} + \lambda_0\varphi^* - \beta_1 T)\,\delta_{ij} + \mu\,(u_{i,j} + u_{j,i}) + k\,(u_{j,i}\,\varepsilon_{ijr}\,\varphi_r), \tag{5}$$

$$m_{ij} = \alpha\,\varphi_{r,r}\delta_{ij} + \beta\,\varphi_{i,j} + \gamma\,\varphi_{j,i}, \tag{6}$$

$$\lambda_k = \alpha_0\,\varphi^*_{,k}, \qquad e = u_{k,k}. \tag{7}$$

From Eq. (1) and Eq. (5) for $\boldsymbol{u}\,(x,z,t) = u\,(u_1, 0, u_3)$ and $\boldsymbol{\Omega} = (0, \Omega, 0)$, the equations of motion can be written as

$$(\lambda+\mu)\,e_{,x} + (\mu+k)\,u_{1,ii} + \lambda_0\,\varphi^*_{,x} - k\,\varphi_{2,z} - \beta_1 T_{,x} = \rho[u_{1,tt} - \Omega^2 u_1 + 2\,\Omega u_{3,t}\,], \tag{8}$$

$$(\lambda+\mu)\,e_{,z} + (\mu+k)\,u_{3,ii} + \lambda_0\,\varphi^*_{,z} - k\,\varphi_{2,x} - \beta_1 T_{,z} = \rho[u_{3,tt} - \Omega^2 u_3 + 2\,\Omega u_{1,t}\,]. \tag{9}$$

From Eqs. (5) and (6) into Eq (2) for $\boldsymbol{\varphi} = (0, \varphi_2, 0)$, the equation of micropolar is given by

$$\gamma\varphi_{2,ii} + k\,(u_{1,z} - u_{3,x}) - 2k\,\varphi_2 = \rho\, j\,\varphi_{2,tt}. \tag{10}$$

We employ the following dimensionless variables

$$(x', z') = \frac{\omega^*}{c_1}(x, z),\quad u_i' = \frac{\rho\,\omega^* c_1 u_i}{\beta_1 T_0},\quad (t', \tau_\nu', \tau_\theta', \tau_q') = \omega^*(t, \tau_\nu, \tau_\theta, \tau_q),\quad \varphi_2' = \frac{\rho c_1^2\,\varphi_2}{\beta_1 T_0},\quad T' = \frac{T}{T_0},$$
$$\varphi^{*\prime} = \frac{\rho c_1^2\varphi^*}{\beta_1 T_0},\quad \sigma_{ij}' = \frac{\sigma_{ij}}{\beta_1 T_0},\quad m_{ij}' = \frac{\omega^* m_{ij}}{c_1\beta_1 T_0},\quad \lambda_k' = \frac{\omega^*\lambda_k}{c_1\beta_1 T_0},\quad \Omega = \frac{\Omega}{\omega^*},\quad c_1^2 = \frac{\lambda + 2\mu + k}{\rho}. \tag{11}$$

After introducing the displacement potentials $\Phi(x, z, t)$ and $\psi(x, z, t)$ which correspond to displacement components, we acquire

$$u_1 = \Phi_{,x} + \psi_{,z}, \quad u_3 = \Phi_{,z} - \psi_{,x}. \tag{12}$$

Substituting Eqs. (11) and (12) in Eqs. (3), (4), (8), (9) and (10), we obtain

$$[(a_1+a_2)\nabla^2+\Omega^2-\frac{\partial^2}{\partial t^2}]\Phi+2\Omega\psi_{,t}+a_3\varphi^*-T=0, \tag{13}$$

$$[a_2\nabla^2+\Omega^2-\frac{\partial^2}{\partial t^2}]\psi-2\Omega\,\Phi_{,t}-a_4\,\varphi_2=0, \tag{14}$$

$$[\nabla^2-2a_5-a_6\frac{\partial^2}{\partial t^2}]\varphi_2+\ a_5\nabla^2\psi=0, \tag{15}$$

$$[a_7\nabla^2-\frac{1}{3}a_3-\frac{3}{2}a_{10}\frac{\partial^2}{\partial t^2}]\varphi^*+\frac{1}{3}a_8T-\frac{1}{3}a_9\nabla^2\Phi=0, \tag{16}$$

$$\nabla^2T+(a_{11}+\tau_\nu)\nabla^2T_{,t}+\tau_\theta a_{11}\nabla^2T_{,tt}=[1+\tau_q\frac{\partial}{\partial t}+\frac{1}{2}\tau_q^2\frac{\partial^2}{\partial t^2}][a_{12}T_{,tt}+a_{13}\varphi^*_{,tt}+a_{14}\nabla^2\Phi_{,tt}]. \tag{17}$$

3. Normal mode analysis

The solution of the considered physical variable can be decomposed in terms of the normal mode method take the following form:

$$[u_i,\Phi,\psi,\varphi^*,\varphi_2,T,\sigma_{ij},m_{ij},u_i^f,\sigma_{ij}^f](x,z,t)=[\bar{u}_i,\bar{\Phi},\bar{\psi},\bar{\varphi}^*,\bar{\varphi}_2,\bar{T},\bar{\sigma}_{ij},\bar{m}_{ij},\bar{u}_i^f,\bar{\sigma}_{ij}^f](z)\,e^{ib(x-\omega t)}. \tag{18}$$

where, ω is the frequency, $i=\sqrt{-1}$ is the complex number and b is the wave number in the $x-$ direction. Using Eq. (18) in Eqs. (13)-(17), we have

$$(\delta_1\mathrm{D}^2+\delta_2)\,\bar{\Phi}-\delta_3\,\bar{\psi}+a_3\bar{\varphi}^*-\bar{T}=0, \tag{19}$$

$$\delta_5\,\bar{\Phi}+(a_2\mathrm{D}^2+\delta_4)\,\bar{\psi}-a_4\bar{\varphi}_2=0, \tag{20}$$

$$(a_5\mathrm{D}^2-a_5b^2)\,\bar{\psi}+(\mathrm{D}^2+\delta_6)\,\bar{\varphi}_2=0, \tag{21}$$

$$(\delta_8\mathrm{D}^2+\delta_9)\,\bar{\Phi}+(a_7\mathrm{D}^2+\delta_7)\,\bar{\varphi}^*+\delta_{10}\bar{T}=0, \tag{22}$$

$$(\delta_{12}\mathrm{D}^2-\delta_{13})\,\bar{\Phi}+\delta_{16}\bar{\varphi}^*+(\delta_{14}\mathrm{D}^2+\delta_{15})\,\bar{T}=0, \tag{23}$$

The existence of non-trivial solutions demands the following necessary and sufficient condition to be hold, i.e., the determinant of the above Eqs. (19-23) needs to be zero, we get

$$(\mathrm{D}^{10}-A\,\mathrm{D}^8+B\,\mathrm{D}^6-C\,\mathrm{D}^4+E\,\mathrm{D}^2-F)\{\bar{\Phi}(z),\bar{\psi}(z),\bar{\varphi}_2(z),\bar{\varphi}^*(z),\bar{T}(z)\}=0. \tag{24}$$

Eq. (24) can be factorized as:

$$(\mathrm{D}^2-k_1^2)(\mathrm{D}^2-k_2^2)(\mathrm{D}^2-k_3^2)(\mathrm{D}^2-k_4^2)(\mathrm{D}^2-k_5^2)\,\{\bar{\Phi}(z),\bar{\psi}(z),\bar{\varphi}_2(z),\bar{\varphi}^*(z),\bar{T}(z)\}=0. \tag{25}$$

where, $k_n^2,(n=1,2,3,4,5)$ are the roots of the characteristic equation of Eq. (25).
The solution of Eq. (25) has the shape:

$$\bar{\Phi}(z)=\sum_{n=1}^{5}M_n\,e^{k_nz}+\sum_{n=1}^{5}M_{n+5}\,e^{-k_nz}, \tag{26}$$

$$\bar{\psi}(z)=\sum_{n=1}^{5}H_{1n}M_n\,e^{k_nz}+\sum_{n=1}^{5}H_{1(n+5)}M_{n+5}\,e^{-k_nz}, \tag{27}$$

$$\bar{\varphi}_2(z)=\sum_{n=1}^{5}H_{2n}M_n\,e^{k_nz}+\sum_{n=1}^{5}H_{2(n+5)}M_{n+5}\,e^{-k_nz}, \tag{28}$$

$$\bar{T}(z)=\sum_{n=1}^{5}H_{3n}M_n\,e^{k_nz}+\sum_{n=1}^{5}H_{3(n+5)}M_{n+5}\,e^{-k_nz}, \tag{29}$$

$$\bar{\varphi}^*(z)=\sum_{n=1}^{5}H_{4n}M_ne^{k_nz}+\sum_{n=1}^{5}H_{4(n+5)}M_{n+5}e^{-k_nz}. \tag{30}$$

Substituting from Eqs. (26) and (27) in Eq. (12) we acquire

$$\bar{u}_1(z)=\sum_{n=1}^{5}[ib+k_nH_{1n}]M_ne^{k_nz}+\sum_{n=1}^{5}[ib-k_nH_{1(n+5)}]M_{n+5}e^{-k_nz}, \tag{31}$$

$$\bar{u}_3(z)=\sum_{n=1}^{5}[k_n-ibH_{1n}]M_n\,e^{k_nz}-\sum_{n=1}^{5}[k_n+ibH_{1(n+5)}]M_{n+5}\,e^{-k_nz}. \tag{32}$$

By compensation from Eqs. (11-18) into Eqs. (5-7) and by using Eqs. (28-32) we infer that the components of the stress tensor, the following components

$$\bar{\sigma}_{xx}(z)=\sum_{n=1}^{5}H_{5n}M_n\,e^{k_n z}+\sum_{n=1}^{5}H_{5(n+5)}M_{n+5}\,e^{-k_n z}, \tag{33}$$

$$\bar{\sigma}_{yy}(z)=\sum_{n=1}^{5}H_{6n}M_n e^{k_n z}+\sum_{n=1}^{5}H_{6(n+5)}M_{n+5}e^{-k_n z}, \tag{34}$$

$$\bar{\sigma}_{zz}(z)=\sum_{n=1}^{5}H_{7n}M_n e^{k_n z}+\sum_{n=1}^{5}H_{7(n+5)}M_{n+5}e^{-k_n z}, \tag{35}$$

$$\bar{\sigma}_{xz}(z)=\sum_{n=1}^{5}H_{8n}M_n e^{k_n z}+\sum_{n=1}^{5}H_{8(n+5)}M_{n+5}e^{-k_n z}, \tag{36}$$

$$\bar{\sigma}_{zx}(z)=\sum_{n=1}^{5}H_{9n}M_n e^{k_n z}+\sum_{n=1}^{5}H_{9(n+5)}M_{n+5}e^{-k_n z}, \tag{37}$$

$$\bar{m}_{xy}(z)=\sum_{n=1}^{5}i\,b\,a_{18}H_{2n}M_n\,e^{k_n z}+\sum_{n=1}^{5}i\,b\,a_{18}H_{2(n+5)}M_{n+5}\,e^{-k_n z}, \tag{38}$$

$$\bar{m}_{yx}(z)=\sum_{n=1}^{5}ib\,a_{19}H_{2n}M_n e^{k_n z}+\sum_{n=1}^{5}ib\,a_{19}H_{2(n+5)}M_{n+5}e^{-k_n z}, \tag{39}$$

$$\bar{m}_{zy}(z)=\sum_{n=1}^{5}a_{18}k_n H_{2n}M_n e^{k_n z}-\sum_{n=1}^{5}a_{18}k_n H_{2(n+5)}M_{n+5}e^{-k_n z}, \tag{40}$$

$$\bar{m}_{yz}(z)=\sum_{n=1}^{5}a_{19}k_n H_{2n}M_n e^{k_n z}-\sum_{n=1}^{5}a_{19}k_n H_{2(n+5)}M_{n+5}e^{-k_n z}, \tag{41}$$

$$\bar{\lambda}_x(z)=\sum_{n=1}^{5}ib\,a_7H_{4n}M_n e^{k_n z}+\sum_{n=1}^{5}ib\,a_7H_{4(n+5)}M_{n+5}e^{-k_n z}, \tag{42}$$

$$\bar{\lambda}_z(z)=\sum_{n=1}^{5}a_7k_nH_{4n}M_ne^{k_n z}-\sum_{n=1}^{5}a_7k_nH_{4(n+5)}M_{n+5}e^{-k_n z}, \tag{43}$$

where the coefficients a_m, $\delta_{m'}$, A, B, C, E, F, $H_{n'n}$, $m=(1,2,......,19)$, $m'=(1,2,......,16)$, $n'=(1,2,.....,9)$ are given in **Appendix.**

The system of governing equation in the fluid is given by Deswal et al. (2022)

$$\lambda^f\ \nabla(\nabla.\boldsymbol{u}^f)=\rho^f\boldsymbol{u}^f_{,tt}, \tag{44}$$

$$\sigma^f_{ij}=\lambda^f u^f_{r,r}\delta_{ij}. \tag{45}$$

Substituting from Eq. (18) into Eqs. (44-45)

$$\Big(\frac{\omega^2 b^2}{c_1^{f\,2}}-b^2\Big)\bar{u}_1^f+i\,b\,\mathrm{D}\,\bar{u}_3^f=0, \tag{46}$$

$$\Big(\mathrm{D}^2+\frac{\omega^2 b^2}{c_1^{f\,2}}\Big)\bar{u}_3^f+ib\,\mathrm{D}\,\bar{u}_1^f=0, \tag{47}$$

where, $c_1^{f\,2}=\dfrac{\lambda^f}{\rho^f}$.

Eliminating $\bar{u}_1^f$, $\bar{u}_3^f$ between Eqs. (46-47), We obtain

$$[\,\mathrm{D}^2-r^2\,](\bar{u}_1^f,\bar{u}_3^f)=0. \tag{48}$$

where $r^2=\Big(b^2-\dfrac{\omega^2 b^2}{c_1^{f\,2}}\Big)$, is the root of the characteristic equation of Eq. (48), the solution of Eq. (48) has the form

$$(\bar{u}_1^f,\bar{u}_3^f)(z)=(1,L_{11})R_1e^{rz}+(1,L_{12})R_2e^{-rz}. \tag{49}$$

Substituting from Eq. (18) in Eq. (45) and by using Eq. (49), we acquire the components of stresses in a fluid layer

$$\bar{\sigma}^f_{xx}(z)=\bar{\sigma}^f_{yy}(z)=\bar{\sigma}^f_{zz}(z)=L_{21}R_1e^{rz}+L_{22}R_2e^{-rz}. \tag{50}$$

Where, $L_{11}=\dfrac{i\,b\,r}{[r^2+\dfrac{\omega^2 b^2}{c_1^{f\,2}}]}$, $L_{12}=\dfrac{-i\,b\,r}{[r^2+\dfrac{\omega^2 b^2}{c_1^{f\,2}}]}$, $L_{21}=\lambda^f[ib+rL_{11}]$, $L_{22}=\lambda^f[ib-rL_{12}]$.

4. Boundary conditions

The boundary conditions for the problem at $z=\pm d$, to determine the constants $M_{i'}$, $i'=(1,2,......,10)$, R_1 and R_2, are

$$\sigma_{xx}=\sigma_{xx}^{f},\ \sigma_{xz}=f_1 e^{ib(x-\omega t)},\ T=f_2 e^{ib(x-\omega t)},\ \frac{\partial u_1}{\partial z}=\frac{\partial u_1^f}{\partial z},\ \varphi^*=0,\ \varphi_2=0 \text{ at } z=\pm d. \tag{51}$$

Using the expressions for σ_{xx}, σ_{xx}^f, σ_{xz}, T, u_1, u_1^f, φ^* and φ_2 in (51), we get

$$\sum_{n=1}^{5} H_{5n}M_n e^{k_n d}+\sum_{n=1}^{5} H_{5(n+5)}M_{n+5} e^{-k_n d}-L_{22}R_2 e^{-rd}=0, \tag{52}$$

$$\sum_{n=1}^{5} H_{5n}M_n e^{-k_n d}+\sum_{n=1}^{5} H_{5(n+5)}M_{n+5} e^{k_n d}-L_{22}R_1 e^{-rd}=0, \tag{53}$$

$$\sum_{n=1}^{5} H_{8n}M_n e^{k_n d}+\sum_{n=1}^{5} H_{8(n+5)}M_{n+5} e^{-k_n d}=f_1, \tag{54}$$

$$\sum_{n=1}^{5} H_{8n}M_n e^{-k_n d}+\sum_{n=1}^{5} H_{8(n+5)}M_{n+5} e^{k_n d}=f_1, \tag{55}$$

$$\sum_{n=1}^{5} [ibk_n+k_n^2 H_{1n}]M_n e^{k_n d}+\sum_{n=1}^{5} [-ibk_n+k_n^2 H_{1(n+5)}]M_{n+5} e^{-k_n d}+rR_2 e^{-rd}=0, \tag{56}$$

$$\sum_{n=1}^{5} [ibk_n+k_n^2 H_{1n}]M_n e^{-k_n d}+\sum_{n=1}^{5} [-ibk_n+k_n^2 H_{1(n+5)}]M_{n+5} e^{k_n d}-rR_1 e^{-rd}=0, \tag{57}$$

$$\sum_{n=1}^{5} H_{3n}M_n e^{k_n d}+\sum_{n=1}^{5} H_{3(n+5)}M_{n+5} e^{-k_n d}=f_2, \tag{58}$$

$$\sum_{n=1}^{5} H_{3n}M_n e^{-k_n d}+\sum_{n=1}^{5} H_{3(n+5)}M_{n+5} e^{k_n d}=f_2, \tag{59}$$

$$\sum_{n=1}^{5} H_{4n}M_n e^{k_n d}+\sum_{n=1}^{5} H_{4(n+5)}M_{n+5} e^{-k_n d}=0, \tag{60}$$

$$\sum_{n=1}^{5} H_{4n}M_n e^{-k_n d}+\sum_{n=1}^{5} H_{4(n+5)}M_{n+5} e^{k_n d}=0, \tag{61}$$

$$\sum_{n=1}^{5} H_{2n}M_n e^{k_n d}+\sum_{n=1}^{5} H_{2(n+5)}M_{n+5} e^{-k_n d}=0, \tag{62}$$

$$\sum_{n=1}^{5} H_{2n}M_n e^{-k_n d}+\sum_{n=1}^{5} H_{2(n+5)}M_{n+5} e^{k_n d}=0. \tag{63}$$

By solving the above system of nonhomogeneous equations, we get the values of constants $M_{i'}$, $i'=(1,2,......,10)$, R_1 and R_2, then, we obtain the distribution of the displacement components u_1, u_3, the temperature T, the scalar micro-stretch φ^*, the microrotation φ_2, the components of the stress σ_{xx}, σ_{yy}, $\sigma_{zz}, \sigma_{xz}, \sigma_{zx}$, the components of couple stress tensor $m_{xy}, m_{yx}, m_{zy}, m_{yz}$, the micro-stress tensor λ_x, λ_z, horizontal displacement for fluid u_1^f, the vertical displacement for fluid u_3^f, the stress components for fluid $\sigma_{xx}^f, \sigma_{yy}^f$ and σ_{zz}^f.

5. Numerical results and discussions

The analysis has been carried out for magnesium crystal-like material (Kumar and Partap, 2009).
$\rho=1.47\times10^{3}\ \text{kg.m}^{-3}$, $\lambda=9.4\times10^{10}\ \text{N.m}^{-2}$, $\mu=4\times10^{10}\ \text{N.m}^{-2}$, $j=0.2\times10^{-19}\ \text{m}^2$, $j_0=1.85\times10^{-19}\ \text{m}^2$, $k=1\times10^{10}\ \text{N.m}^{-2}$, $\alpha_0=0.779\times10^{-9}\ \text{N}$, $\lambda_1=0.5\times10^{10}\ \text{N.m}^{-2}$, $\gamma=0.779\times10^{-9}\ \text{N}$, $T_0=298^\circ\ \text{K}$, $\lambda_0=0.5\times10^{10}\ \text{N.m}^{-2}$, $\beta_1=2.68\times10^{6}\ \text{N.m}^{-2}.\text{k}^{-1}$, $\nu=2\times10^{6}\ \text{N.m}^{-2}.\text{k}^{-1}$, $c_E=1.04\times10^{3}\ \text{J.kg}^{-1}.\text{k}^{-1}$, $k_1^*=1.7\times10^{2}\ \text{J.m}^{-1}.\text{s}^{-1}.\text{k}^{-1}$, $\tau_\nu=0.0171\text{s}$, $\tau_\theta=0.031\text{s}$, $\tau_q=0.5\text{s}$, $\omega_0=1.90013$, $\zeta=5.90018$, $\omega=\omega_0+i\,\zeta$, $b=1$, $d=2$, $f_1=0.0201$, $f_2=1.0502$.

As non-viscous fluid, the physical constants for water are given by Othman and Ismail (2022)

$$\lambda^f = 2.25\times 10^9 \text{ N.m}^{-2}, \ \rho^f = 10^3 \text{ kg.m}^{-3}.$$

In this work, the computations are carried out for the dimensionless time value $t = 0.18$ on the range $-2 \le z \le 2$ on the surface $x = 2.18$ on all physical quantities. The numerical technique presented here is used to explain the variation of the physical quantities u_1, u_3, φ^*, φ_2, σ_{xx} and σ_{xz} with the distance z. The graphs depict the theory of G-N III and the model of 3PHL predicted curves. Figs. 2-7 depict a comparison between the theory of G-N III and the model of 3PHL in the presence and complete absence of rotation. Fig. 2 describes the variation of u_1 versus the distance z. It is noticeable that the values of u_1 based on the theory of the G-N III are greater than the same values based on the model of 3PHL at the two cases $(\Omega = 0,1)$ along the distance z. Fig. 3 shows the variation of u_3 versus the distance z. In the case of the presence of rotation, the two curves that represent the two theories begin with positive values, then decrease to vanish over the rang $-2 \le z \le 0$, and then increase again over the rang $0 \le z \le 2$, whereas, in the absence of rotation, they begin with positive values and increase along the distance z. Fig. 4 depicts the distribution of scalar micro-stretch φ^* against z. It is clarified that the values of φ^* based on the theory of the G-N III are smaller than the same values based on the model of 3PHL at the two cases ($\Omega = 0,1$) along the distance z. Fig. 5 clarifies the effect of rotation on the variation of the microrotation φ_2 against z. In the presence of rotation, the two curves that represent the two theories begin at zero and increase to a maximum value, then decrease up to zero over range $-2 \le z \le 0$, then decrease to a minimum value and increase up to zero over range $0 \le z \le 2$. Fig. 6 exhibits the distribution of σ_{xx} with a distance z. It is noticeable that the values of σ_{xx} on both theories 3PHL and G-N III in the presence of rotation are smaller than the same values in the absence of rotation over the range $-2 \le z \le -1$, and $1 \le z \le 1.5$. Fig. 7 illustrates the distribution of σ_{xx} with a distance z. It is clarified that the values σ_{xx} dependent on the 3PHL model are smaller than the same values dependent on the G-N III theory in the presence pf rotation over the range $-2 \le z \le -1.7$ and $0.7 \le z \le 2$, while the opposite occurs over the range $-1.7 \le z \le 0$.

Figs. 8-13 are represented to illustrate the variation of the above quantities against z, in the presence of rotation $\Omega = 1$ on the model of 3PHL for the different wave number b values. These values are as follows $b = 0.9, b = 1$ and $b = 1.1$. Fig. 8 demonstrates the influence of the wave number b on u_1. It is observed that the values of u_1 increase with the increase of the wave number b over the range $-2 \le z \le -1.5$ and $1 \le z \le 1.5$, while the opposite occurs over the range $-1.5 \le z \le -0.5$. Fig. 9 shows the influence of the wave number b on the vertical displacement u_3. It is clarified that the values of u_3 decrease with the increase of the wave number b on the range $-2 \le z \le -1.4$, After that, there is no difference between the three values of the wave number b. Fig. 10 shows the influence of the wave number b on the scalar micro-stretch φ^*. It is observed that the values of φ^* increase with the decrease of the wave number b. on the range $-2 \le z \le -1.75$ and $1.75 \le z \le 2$, while the opposite occurs on the range $-1.75 \le z \le -1$ and $1 \le z \le 1.75$. Fig. 11 illustrates the effect of the wave number b on the microrotation φ_2. With an increased the wave number b, the values of φ_2 increase on the range $-2 \le z \le -1.8$ and $1 \le z \le 2$. Fig. 12 clarifies the influence of the wave number b on the stress component σ_{xx}. With an decreased the wave number b, the values of φ_2 decrease on the range $-2 \le z \le -1.4$ and $1 \le z \le 2$. Fig. 13 exhibits the variation of stress component σ_{xz} versus z under the effect of the wave number b. It is clarified that the values of σ_{xz} decrease with the increase of the wave number b on the range $-2 \le z \le -1.5$ and $1 \le z \le 2$, while the opposite occurs on the range $-1.5 \le z \le -0.5$. Figs. 14-19 are graphed to describe and demonstrate the distribution of the above quantities versus z, in the presence of rotation $\Omega = 1$ on the model of 3PHL for the different values of the real part of the frequency ω_0. These values are as follows $\omega_0 = 1, \omega_0 = 2$ $\omega_0 = 3$. Figs. 14, 15, 16 and 18 show the effect of the real part of the frequency ω_0 on u_1, u_3, φ^* and σ_{xx}. It is observed that the values of u_1, u_3, φ^* and σ_{xx} increase with the decrease of the real part of the frequency ω_0. Fig. 17 demonstrates the variation of microrotation φ_2 versus z under the effect of the real part of the frequency ω_0. It is noticed that the values of φ_2 increase with the increase of the real part of frequency ω_0 on the range $-1.9 \le z \le -1.6$ and $1.1 \le z \le 1.6$, while the inverse occurs on the range $-1.6 \le z \le -1$ and $1.6 \le z \le 2$. Fig. 19 illustrates the influence of the real part of the frequency ω_0 on the stress component σ_{xz}. It is clarified that the values of σ_{xz} decrease with the decrease of the real part of frequency ω_0 on the range $-2 \le z \le -1.7$, $-1.5 \le z \le -0.1$ and $1.8 \le z \le 2$, while the inverse occurs on the range $-1.7 \le z \le -1.5$ and $0.1 \le z \le 1.8$.

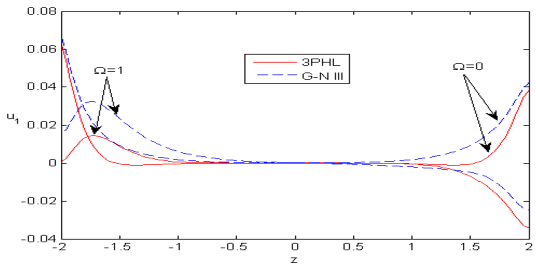

Fig. 2. Variation of the horizontal displacement u_1 against z.

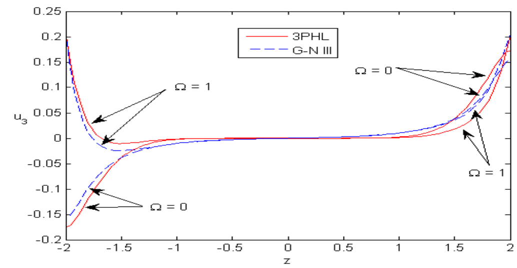

Fig. 3. Variation of the vertical displacement u_3 against z.

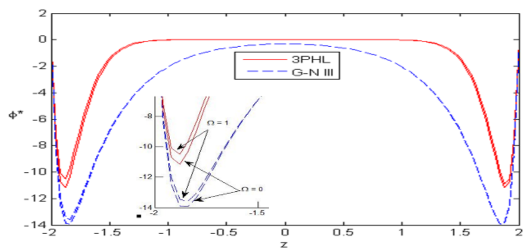

Fig. 4. Variation of the scalar microstretch φ^* against z.

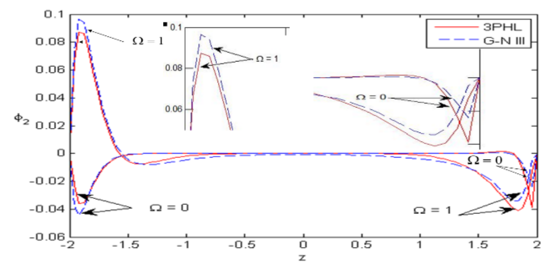

Fig. 5. Variation of the microrotation φ_2 against z.

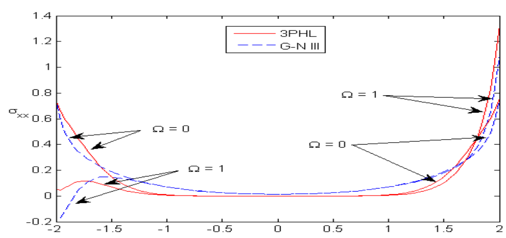

Fig. 6. Variation of the stress component σ_{xx} against z.

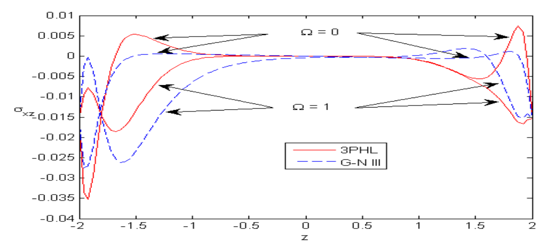

Fig. 7. Variation of the stress component σ_{xz} against z.

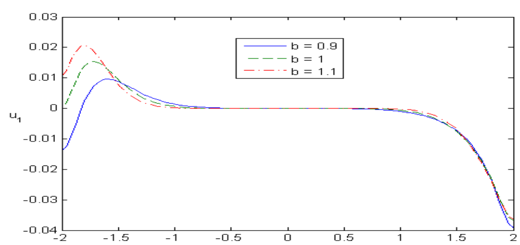

Fig. 8. Influence of wave number b on the distribution of u_1 in the presence of rotation $(\Omega=1)$ on (3PHL) model.

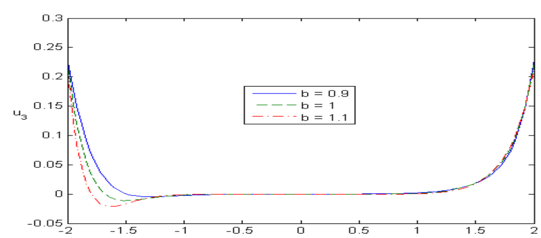

Fig. 9. Influence of wave number b on the distribution u_3 in the presence of rotation $(\Omega=1)$ on (3PHL) model.

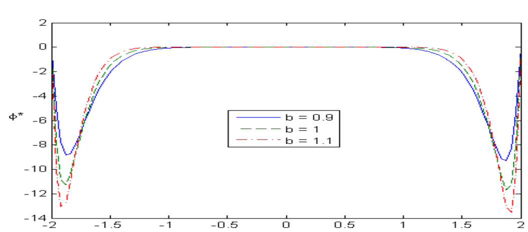

Fig. 10. Influence of wave number b on the distribution of scalar microstretch φ^* in the presence of rotation $(\Omega=1)$ on (3PHL) model.

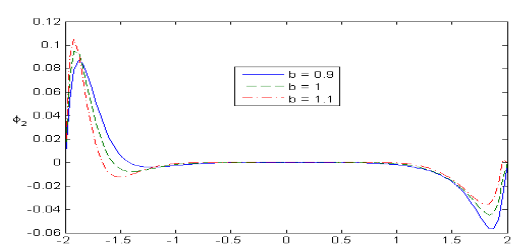

Fig. 11. Influence of wave number b on the distribution of microrotation φ_2 in the presence of rotation $(\Omega=1)$ on (3PHL) model.

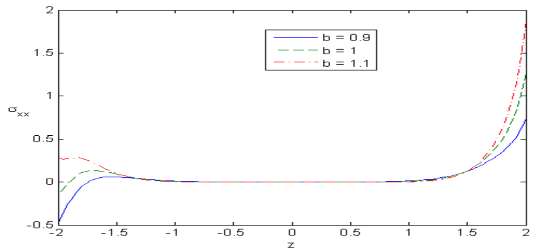

Fig. 12. Influence of wave number b on the distribution of stress component σ_{xx} in the presence of rotation $(\Omega = 1)$ on (3PHL) model.

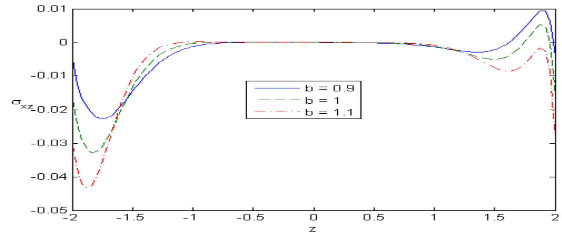

Fig. 13. influence of wave number b on the distribution of stress component σ_{xz} in the presence of rotation $(\Omega = 1)$ on (3PHL) model.

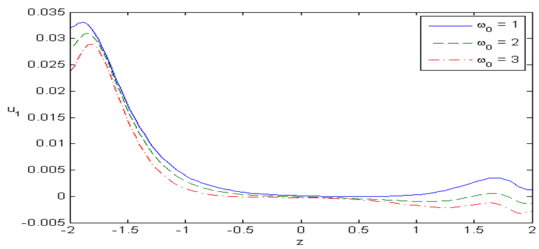

Fig. 14. Effect of real part of frequency ω_0 on the variation of u_1 in the presence of rotation $(\Omega = 1)$ on (3PHL) model.

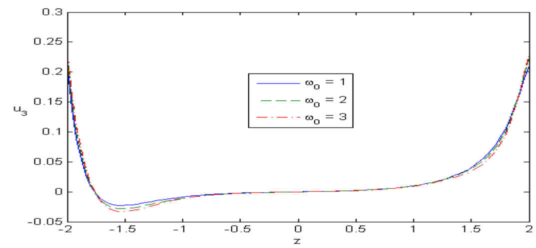

Fig. 15. Effect of real part of frequency ω_0 on the variation of u_3 in the presence of rotation $(\Omega = 1)$ on (3PHL) model.

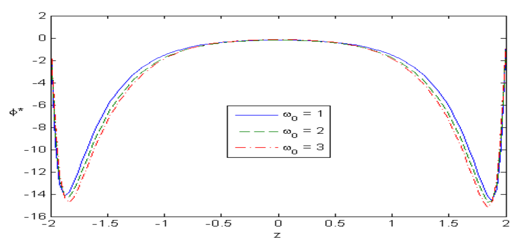

Fig. 16. Effect of real part of frequency ω_0 on the variation of scalar microstretch φ^* in the presence of rotation $(\Omega = 1)$ on (3PHL) model.

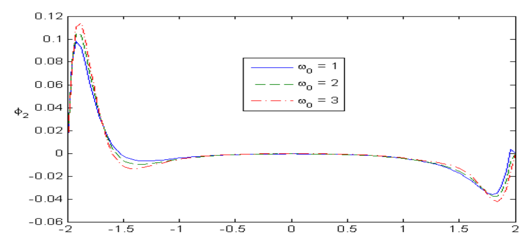

Fig. 17. Effect of real part of frequency ω_0 on the variation of microrotation φ_2 in the presence of rotation $(\Omega = 1)$ on (3PHL) model.

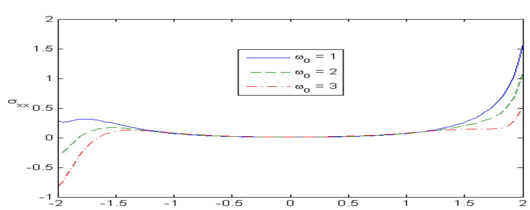

Fig. 18. Effect of real part of frequency ω_0 on the variation of stress component σ_{xx} in the presence of rotation $(\Omega = 1)$ on (3PHL) model.

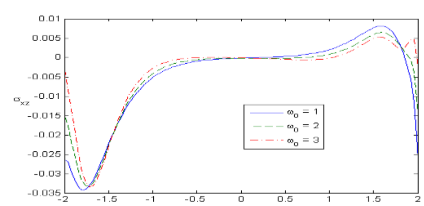

Fig. 19. Effect of real part of frequency ω_0 on the variation of stress component σ_{xz} in the presence of rotation $(\Omega = 1)$ on (3PHL) model.

6. Conclusion

In this paper, the problem of the thermoelastic response in a micro-stretch thermoelastic half-space submerged in an unlimited non-viscous fluid under rotation is considered by employing the theory of G-N III and the model of 3PHL. Utilizing the normal mode analysis, the problem has been solved, from the results discussed above, it can be concluded that:

1- The influence of rotation plays a pivotal role in this study of thermoelastic solid distortion.
2- A comparison is made among the theory of G-N III and the model of 3PHL in the presence and complete absence of rotation.
3- A significant influence of thicknesses of fluid layers is also observed in micro-stretch thermoelastic solids. These results can be exploited in designing different devices in contact with the liquid.
4- The physical quantities are satisfying all the boundary conditions.
5- The wave number and the real part of the frequency parameter have a significant influence on all the physical quantities.

6- The study can be applied in the fields of seismology, geomechanics, earthquake, earthquake engineering, solid dynamics, etc.

Funding

The author received no financial support for the research, authorship, and/or publication of this article.

Conflict of interest

The authors declare that they have no conflict of interest.

Ethical approval

This article does not contain any studies with human participants or animals performed by any of the authors.

References

Abouelregal, A.E., Marin, M., & Askar, S. (2021). Thermo-optical mechanical waves in a rotating solid semiconductor sphere using the improved Green–Naghdi III model. *Mathematics, 9*(22), 2902.

Abouelregal, A. E., Sedighi, H. M., & Shirazi, A. H. (2022). The effect of excess carrier on a semiconducting semi-infinite medium subject to a normal force by means of Green and Naghdi approach. *Silicon, 14*(9), 4955-4967.

Deswal, S., Sheoran, D., Thakran, S., & Kalkal, K. K. (2022). Reflection of plane waves in a nonlocal microstretch thermoelastic medium with temperature dependent properties under three-phase-lag model. *Mechanics of Advanced Materials and Structures, 29*(12), 1692-1707.

Kumar, R., & Partap, G. (2009). Wave propagation in microstretch thermoelastic plate bordered with layers of inviscid liquid. *Multidiscipline Modeling in Materials and Structures, 5*, 171-184.

Kumar, S., Sharma, J. N., & Sharma, Y. D. (2011). Generalized thermoelastic waves in micro-stretch plates loaded with fluid of varying temperature. *International Journal of Applied Mechanics, 3*(3), 563-586.

Kumar, R., & Chawla, V. (2011). A study of plane wave propagation in anisotropic three-phase-lag and two-phase-lag model. *International Communications in Heat and Mass Transfer, 38*(9), 1262-1268.

Kumar, R., Ahuja, S., & Garg, S. K. (2014). Surface wave propagation in a micro-stretch thermoelastic diffusion material under an inviscid liquid layer. *Advances in Acoustics and Vibration,* 2014.

Kumar, R. (2015). Wave propagation in a microstretch thermoelastic diffusion solid. Analele ştiinţifice ale Universităţii "Ovidius" Constanţa. *Seria Matematică, 23*(1), 127-170.

Kutbi, M. A., & Zenkour, A. M. (2021) Thermomechanical waves in an axi-symmetric rotating disk using refined Green–Naghdi models. *International Journal of Applied Mechanics, 13*(03), 2150035.

Lata, P., & Himanshi, H. (2022). Fractional effect in an orthotropic magneto-thermo-elastic rotating solid of type GN-II due to normal force. *Structural Engineering and Mechanics, 81*(4), 503-511.

Marin, M., & Öchsner, A. (2018) An initial boundary value problem for modeling a piezoelectric dipolar body. *Continuum Mechanics and Thermodynamics, 30*, 267–278.

Marin, M., Öchsner, A. & Taus, D. (2020) On structural stability for an elastic body with voids having dipolar structure. *Continuum Mechanics and Thermodynamics, 32*, 147–160.

Marin, M., Ochsner, A., & Othman, M. I. A. (2022). On the evolution of solutions of mixed problem in thermoelasticity of porous bodies with dipolar structure. *Continuum Mechanics and Thermodynamics, 34*(2), 491-506

Miszuris, W., & Öchsner, A. (2013). Universal transmission conditions for thin reactive heat-conducting interphases. *Continuum Mechanics and Thermodynamics, 25*, 1–21.

Othman, M. I. A., & Atwa, S. Y. (2014). Effect of rotation on a fiber-reinforced thermo-elastic under Green-Naghdi theory and influence of gravity. *Meccanica, 49*(1), 23-36.

Othman, M. I. A., Said, S. M., & Marin, M. (2019). A novel model of plane waves of two-temperature fiber-reinforced thermoelastic medium under the effect of gravity with three-phase-lag model. *International Journal of Numerical Methods for Heat and Fluid Flow, 29*(12), 4788-4806.

Othman, M. I. A., Atwa, S. Y., Eraki, E. E., & Ismail, M. F. (2021). The initial stress effect on a thermoelastic micro-elongated solid under the dual-phase-lag model. *Applied Physics A., 127*(9), 1-8.

Othman, M. I. A., & Abbas, I. A. (2021). 2-D problem of micropolar thermoelastic rotating medium with eigenvalue approach under the three-phase-lag model. *Waves Random Complex Media*. DOI: 10.1080/17455030.2021.1879405

Othman, M. I. A., Atwa, S. Y., Eraki, E. E., & Ismail, M. F. (2021). A thermoelasticmicro-elongated layer under the effect of gravity in the context of the dual-phase lag model. *Journal of Applied Mathematics and Mechanics, 101*(12), e202100109

Othman, M. I. A., Ismail, M. F. (2022). The gravitational field effect on a micro-elongated thermoelastic layer under the fluid load, using the lord-shulman theory and dual-phase-lag model. *Multidiscipline Modeling in Materials and Structures, 18*(5), 757-771.

Roy Choudhuri, S. K. (2007). On a thermoelastic three-phase-lag model. *Journal of Thermal Stresses, 30*(3), 231-238.

Sharma, J. N., Kumar, S., & Sharma, Y. D. (2007) Propagation of Rayleigh surface waves in microstretch thermoelastic continua under inviscid fluid loadings. *Journal of Thermal Stresses, 31*(1), 18-39

Sharma, D. K., Sharma, M. K., & Sarkar, N. (2021). Effect of three-phase-lag model on the analysis of three-dimensional free vibrations of viscothermoelastic solid cylinder. *Applied Mathematical Modelling, 90*, 281-301.

Singh, B., & Singla, H. (2020). The effect of rotation on the propagation of waves in an incompressible transversely isotropic thermoelastic solid. *Acta Mechanica, 231*(1), 2485-2495.

Sur, A., & Kanoria, M. (2014) Thermoelastic interaction in a viscoelastic functionally graded half-space under three-phase-lag model. *European Journal of Computational Mechanics, 23*(5-6), 179-198.

Sur, A. (2022). Memory responses in a three-dimensional thermo-viscoelastic medium. *Waves Random Complex Media, 32*(1), 137-154.

Xu, C. G., Xu, B. Q., & Xu, G. D. (2011). Laser-induced thermoelastic Leaky Lamb waves at the fluid–solid interface. *Applied Physics A., 105*(2), 379-386.

Youssef, H. M., & El-Bary, A. A. (2022) Characterization of the photothermal interaction of a semiconducting solid sphere due to the mechanical damage and rotation under Green-Naghdi theories. *Mechanics of Advanced Materials and Structures, 29*(6), 889-904.

Appendix

$$a_1 = \frac{\lambda+\mu}{\rho c_1^2},\ a_2 = \frac{\lambda+k}{\rho c_1^2},\ a_3 = \frac{\lambda_0}{\rho c_1^2},\ a_4 = \frac{k}{\rho c_1^2},\ a_5 = \frac{k c_1^2}{\gamma \omega^{*2}},\ a_6 = \frac{\rho j c_1^2}{\gamma},\ a_7 = \frac{\alpha_0 \omega^{*2}}{\rho c_1^4},\ a_8 = \frac{\nu}{\beta_1},\ a_9 = \frac{\lambda_0}{\rho c_1^2},\ a_{10} = \frac{j_0 \omega^{*2}}{c_1^2},$$

$$a_{11} = \frac{k_1^* \omega^*}{k^*},\ a_{12} = \frac{\rho c_E c_1^2}{k^*},\ a_{13} = \frac{\nu T_0 \beta_1}{\rho k^*},\ a_{14} = \frac{\beta_1^2 T_0}{\rho k^*},\ a_{15} = \frac{\lambda}{\rho c_1^2},\ a_{16} = \frac{2\mu + k}{\rho c_1^2},\ a_{17} = \frac{\mu}{\rho c_1^2},\ a_{18} = \frac{\gamma \omega^{*2}}{\rho c_1^4},\ a_{19} = \frac{\beta \omega^{*2}}{\rho c_1^4},$$

$$\delta_1 = (a_1 + a_2),\quad \delta_2 = -b^2 \delta_1 + b^2 \omega^2 + \Omega^2,\quad \delta_3 = 2ib\,\omega\Omega,\quad \delta_4 = b^2\omega^2 - a_2 b^2 + \Omega^2,\quad \delta_5 = \delta_3,\quad \delta_6 = a_6 b^2 \omega^2 - 2a_5 - b^2,$$

$$\delta_7 = \frac{3}{2} a_{10} b^2 \omega^2 - a_7 b^2 - \frac{1}{3} a_3,\quad \delta_8 = -\frac{1}{3} a_9,\quad \delta_9 = -\delta_8 b^2,\quad \delta_{10} = \frac{1}{3} a_8,\quad \delta_{11} = 1 - ib\omega\tau_q - \frac{1}{2} b^2 \omega^2 \tau_q^2,\quad \delta_{12} = a_{14} b^2 \omega^2,$$

$$\delta_{13} = a_{14} b^4 \omega^2,$$

$$\delta_{14} = 1 - ib\omega(a_{11} + \tau_\nu) - \tau_\theta a_{11} b^2 \omega^2,\ \delta_{15} = i(a_{11} + \tau_\nu) b^3 \omega + \tau_\theta a_{11} b^4 \omega^2 + \delta_{11} a_{12} b^2 \omega^2,\ \delta_{16} = \delta_{11} a_{13} b^2 \omega^2,$$

$$A = \left(\frac{-1}{a_2 a_7 \delta_1 \delta_{14}}\right)[\, a_2 a_7 \delta_{12} + a_2 a_7 \delta_1 \delta_{15} + a_2 a_7 \delta_2 \delta_{14} + a_2 \delta_1 \delta_7 \delta_{14} + a_7 \delta_1 \delta_4 \delta_{14} + a_4 a_5 a_7 \delta_1 \delta_{14} + a_2 a_7 \delta_1 \delta_6 \delta_{14} - a_2 a_3 \delta_8 \delta_{14}],$$

$$\begin{aligned} B = \left(\frac{1}{a_2 a_7 \delta_1 \delta_{14}}\right)[\, & a_2 \delta_7 \delta_{12} - a_2 a_7 \delta_{13} + a_7 \delta_4 \delta_{12} - a_2 \delta_8 \delta_{16} + a_4 a_5 a_7 \delta_{12} + a_2 a_7 \delta_2 \delta_{15} + a_2 a_3 \delta_{10} \delta_{12} + a_2 a_7 \delta_6 \delta_{12} \\ & - a_2 a_3 \delta_8 \delta_{15} - a_2 a_3 \delta_9 \delta_{14} + a_2 \delta_1 \delta_7 \delta_{15} + a_2 \delta_2 \delta_7 \delta_{14} + a_7 \delta_1 \delta_4 \delta_{15} + a_7 \delta_2 \delta_4 \delta_{14} - a_2 \delta_1 \delta_{10} \delta_{16} + a_7 \delta_3 \delta_5 \delta_{14} \\ & + \delta_1 \delta_4 \delta_7 \delta_{14} + a_4 a_5 a_7 \delta_1 \delta_{15} + a_4 a_5 a_7 \delta_2 \delta_{14} + a_4 a_5 a_7 \delta_2 \delta_{14} - a_3 \delta_4 \delta_8 \delta_{14} + a_2 a_7 \delta_2 \delta_6 \delta_{14} + a_4 a_5 \delta_1 \delta_7 \delta_{14} - a_2 a_3 \delta_6 \delta_8 \delta_{14} \\ & + a_2 \delta_1 \delta_6 \delta_7 \delta_{14} + a_7 \delta_1 \delta_4 \delta_6 \delta_{14} - a_4 a_5 a_7 b^2 \delta_1 \delta_{14} - a_3 a_4 a_5 \delta_8 \delta_{14} + a_2 a_7 \delta_1 \delta_6 \delta_{15}], \end{aligned}$$

$$\begin{aligned} C = \left(\frac{-1}{a_2 a_7 \delta_1 \delta_{14}}\right)[\, & - a_2 \delta_7 \delta_{13} - a_7 \delta_4 \delta_{13} - a_2 \delta_9 \delta_{16} + \delta_4 \delta_7 \delta_{12} - \delta_4 \delta_8 \delta_{16} - a_4 a_5 a_7 \delta_{13} - a_2 a_3 \delta_{10} \delta_{13} - a_2 a_7 \delta_6 \delta_{13} \\ & - a_2 a_3 \delta_9 \delta_{15} - a_4 a_5 \delta_8 \delta_{16} + a_2 \delta_2 \delta_7 \delta_{15} + a_2 \delta_6 \delta_7 \delta_{12} + a_7 \delta_2 \delta_4 \delta_{15} + a_7 \delta_4 \delta_6 \delta_{12} - a_2 \delta_2 \delta_{10} \delta_{16} - a_3 \delta_4 \delta_8 \delta_{15} \\ & - a_3 \delta_4 \delta_9 \delta_{14} + a_7 \delta_3 \delta_5 \delta_{15} - a_2 \delta_6 \delta_8 \delta_{16} + \delta_1 \delta_4 \delta_7 \delta_{15} + \delta_2 \delta_4 \delta_7 \delta_{14} + \delta_3 \delta_5 \delta_7 \delta_{14} - \delta_1 \delta_4 \delta_{10} \delta_{16} + a_4 a_5 a_7 \delta_2 \delta_{15} \\ & + a_3 a_4 a_5 \delta_{10} \delta_{12} - a_3 a_4 a_5 \delta_8 \delta_{15} - a_3 a_4 a_5 \delta_9 \delta_{14} + a_2 a_7 \delta_2 \delta_6 \delta_{15} + a_4 a_5 \delta_1 \delta_7 \delta_{15} + a_4 a_5 \delta_2 \delta_7 \delta_{14} + a_2 a_3 \delta_6 \delta_{10} \delta_{12} \\ & - a_2 a_3 \delta_6 \delta_8 \delta_{15} - a_2 a_3 \delta_6 \delta_9 \delta_{14} - a_4 a_5 \delta_1 \delta_{10} \delta_{16} + a_2 \delta_1 \delta_6 \delta_7 \delta_{15} + a_2 \delta_2 \delta_6 \delta_7 \delta_{14} + a_7 \delta_1 \delta_4 \delta_6 \delta_{15} + a_7 \delta_2 \delta_4 \delta_6 \delta_{14} \\ & - a_2 \delta_1 \delta_6 \delta_{10} \delta_{16} - a_3 \delta_4 \delta_6 \delta_8 \delta_{14} + a_7 \delta_3 \delta_5 \delta_6 \delta_{14} + \delta_1 \delta_4 \delta_6 \delta_7 \delta_{14} - a_4 a_5 a_7 b^2 \delta_{12} - a_4 a_5 a_7 b^2 \delta_1 \delta_{15} - a_4 a_5 a_7 b^2 \delta_2 \delta_{14} \\ & + a_3 a_4 a_5 b^2 \delta_8 \delta_{14} - a_4 a_5 b^2 \delta_1 \delta_7 \delta_{14} + a_4 a_5 \delta_7 \delta_{12}], \end{aligned}$$

$$\begin{aligned} E = \left(\frac{1}{a_2 a_7 \delta_1 \delta_{14}}\right)[\, & - \delta_4 \delta_7 \delta_{13} - \delta_4 \delta_9 \delta_{16} - a_4 a_5 \delta_7 \delta_{13} - a_4 a_5 \delta_9 \delta_{16} - a_2 \delta_6 \delta_7 \delta_{13} - a_3 \delta_4 \delta_{10} \delta_{13} - a_7 \delta_4 \delta_6 \delta_{13} - a_3 \delta_4 \delta_9 \delta_{15} \\ & - a_2 \delta_6 \delta_9 \delta_{16} + \delta_2 \delta_4 \delta_7 \delta_{15} + \delta_4 \delta_6 \delta_7 \delta_{12} + \delta_3 \delta_4 \delta_7 \delta_{15} - \delta_2 \delta_4 \delta_{10} \delta_{16} - \delta_3 \delta_5 \delta_{10} \delta_{16} - \delta_4 \delta_6 \delta_8 \delta_{16} - a_3 a_4 a_5 \delta_{10} \delta_{13} \\ & - a_3 a_4 a_5 \delta_9 \delta_{15} + a_4 a_5 \delta_2 \delta_7 \delta_{15} - a_2 a_3 \delta_6 \delta_{10} \delta_{13} - a_2 a_3 \delta_6 \delta_9 \delta_{15} - a_4 a_5 \delta_2 \delta_{10} \delta_{16} + a_2 \delta_2 \delta_6 \delta_7 \delta_{15} + a_7 \delta_2 \delta_4 \delta_6 \delta_{15} \\ & + a_3 \delta_4 \delta_6 \delta_{10} \delta_{12} - a_2 \delta_2 \delta_6 \delta_{10} \delta_{16} - a_3 \delta_4 \delta_6 \delta_8 \delta_{15} - a_3 \delta_4 \delta_6 \delta_9 \delta_{14} + a_7 \delta_3 \delta_5 \delta_6 \delta_{15} + \delta_1 \delta_4 \delta_6 \delta_7 \delta_{15} + \delta_2 \delta_4 \delta_6 \delta_7 \delta_{14} \\ & + \delta_3 \delta_5 \delta_6 \delta_7 \delta_{14} - \delta_1 \delta_4 \delta_6 \delta_{10} \delta_{16} + a_4 a_5 a_7 b^2 \delta_{13} - a_4 a_5 b^2 \delta_7 \delta_{12} + a_4 a_5 b^2 \delta_8 \delta_{16} - a_4 a_5 a_7 b^2 \delta_2 \delta_{15} - a_3 a_4 a_5 b^2 \delta_{10} \delta_{12} \\ & + a_3 a_4 a_5 b^2 \delta_8 \delta_{15} + a_3 a_4 a_5 b^2 \delta_9 \delta_{14} - a_4 a_5 b^2 \delta_1 \delta_7 \delta_{15} - a_4 a_5 b^2 \delta_2 \delta_7 \delta_{14} + a_4 a_5 b^2 \delta_1 \delta_{10} \delta_{16}], \end{aligned}$$

$$F=\left(\frac{1}{a_2a_7\delta_1\delta_{14}}\right)[-\delta_4\delta_6\delta_9\delta_{16}-\delta_4\delta_6\delta_7\delta_{13}-a_3\delta_4\delta_6\delta_{10}\delta_{13}-a_3\delta_4\delta_6\delta_9\delta_{15}+\delta_2\delta_4\delta_6\delta_7\delta_{15}+\delta_3\delta_5\delta_6\delta_7\delta_{15}-\delta_2\delta_4\delta_6\delta_{10}\delta_{16}$$
$$-\delta_3\delta_5\delta_6\delta_{10}\delta_{16}+a_4a_5b^2\delta_7\delta_{13}+a_4a_5b^2\delta_9\delta_{16}+a_3a_4a_5b^2\delta_{10}\delta_{13}+a_3a_4a_5b^2\delta_9\delta_{15}-a_4a_5b^2\delta_2\delta_7\delta_{15}+a_4a_5b^2\delta_2\delta_{10}\delta_{16}],$$

$$H_{1n}=H_{1(n+5)}=\frac{-\delta_5(k_n^2+\delta_6)}{a_2k_n^2+(a_4a_5+\delta_4+a_2\delta_6)k_n^2+\delta_4\delta_6-a_4a_5b^2},\quad H_{2n}=H_{2(n+5)}=\frac{-(a_5k_n^2-a_5b^2)H_{1n}}{k_n^2+\delta_6},$$

$$H_{3n}=H_{3(n+5)}=\frac{k_n^2(\delta_1\delta_{16}-a_3\delta_{12})+a_3\delta_{13}+\delta_2\delta_{16}-\delta_3\delta_{16}H_{1n}}{a_3\delta_{14}k_n^2+\delta_{16}+a_3\delta_{15}},\ H_{4n}=H_{4(n+5)}=\frac{-\delta_8k_n^2-\delta_9-\delta_{10}H_{3n}}{a_7k_n^2+\delta_7},$$
$$H_{5n}=ib(a_{15}+a_{16})[ib+k_nH_{1n}]+a_{15}(k_n^2-ibk_nH_{1n})+a_3H_{4n}-H_{3n},$$
$$H_{5(n+5)}=ib(a_{15}+a_{16})(ib-k_nH_{1(n+5)})+a_{15}(k_n^2-ibk_nH_{1(n+5)})+a_3H_{4(n+5)}-H_{3(n+5)},$$
$$H_{6n}=iba_{15}(ib+k_nH_{1n})+a_{15}(k_n^2-ibk_nH_{1n})+a_3H_{4n}-H_{3n},$$
$$H_{6(n+5)}=iba_{15}(ib-k_nH_{1(n+5)})+a_{15}(k_n^2+ibk_nH_{1(n+5)})+a_3H_{4(n+5)}-H_{3(n+5)},$$
$$H_{7n}=iba_{15}(ib+k_nH_{1n})+(a_{15}+a_{16})(k_n^2-ibk_nH_{1n})+a_3H_{4n}-H_{3n},$$
$$H_{7(n+5)}=iba_{15}(ib-k_nH_{1(n+5)})+(a_{15}+a_{16})(k_n^2+ibk_nH_{1(n+5)})+a_3H_{4(n+5)}-H_{3(n+5)},$$
$$H_{8n}=a_{17}(ibk_n+k_n^2H_{1n})+iba_2(k_n-ibH_{1n})+a_4H_{2n},\ H_{8(n+5)}=a_{17}(-ibk_n+k_n^2H_{1(n+5)})-iba_2(k_n+ibH_{1(n+5)})+a_4H_{2(n+5)},$$
$$H_{9n}=a_2(ibk_n+k_n^2H_{1n})+iba_{17}(k_n-ibH_{1n})-a_4H_{2n},\ H_{9(n+5)}=a_2(-ibk_n+k_n^2H_{1(n+5)})-iba_{17}(k_n+ibH_{1(n+5)})-a_4H_{2(n+5)}.$$